Interference Alignment for Heterogeneous Full-duplex Cellular Networks

Amr El-Keyi and Halim Yanikomeroglu

Department of Systems and Computer Engineering, Carleton University, Ottawa, Ontario, Canada.
Email: amr.elkeyi@sce.carleton.ca, halim.yanikomeroglu@sce.carleton.ca

***Abstract*—In this paper, we consider a heterogeneous network composed of a full-duplex macrocell and a half-duplex femtocell. The macro-base station (BS) is equipped with L antennas where each antenna can be utilized either for downlink transmission or uplink reception. On the other hand, the femto-BS is equipped with M antennas that are used for downlink transmission. We assume that each user equipment has N antennas where $L > M \geq N$. We investigate the benefit of using interference alignment for cross-tier and full-duplex interference management and present precoding schemes that are capable of achieving the total degrees of freedom of the network. We show that full-duplex operation of the macro-BS improves the degrees of freedom (DoF) of the system when $M < 2N$, otherwise half-duplex operation is optimal. Furthermore, the DoF of the system can be improved by 50% via full-duplex macro-BS operation when $M = N$.**

***Index Terms*—Interference alignment, degrees of freedom, separate-antenna full-duplex transceivers, heterogeneous networks, cross-tier interference mitigation.**

I. Introduction

In-band full-duplex (IBFD) transmission brings many advantages to cellular communication systems. It can increase the number of interference-free data streams transmitted in the network and reduce the delay in the feedback of control information, channel state information and acknowledgment messages [1]. However, IBFD transmission poses several challenges from the implementation, physical layer, and medium access control layer perspectives [2]. For example, simultaneous in-band transmission and reception from a single node causes the transmitted signals to loop back to the receiver causing self-interference [3]. In addition, IBFD transmission increases the inter-user interference due to increasing the number of simultaneous transmissions from the network nodes.

In order to utilize IBFD transceivers in cellular systems, self-interference suppression by more than 106 dB is required [4]. Full-duplex transceivers employ either shared or separate antennas for simultaneous IBFD transmission and reception. Separate-antenna IBFD transceivers are more likely to be implemented in cellular systems as they divide the available antennas into two groups; one for transmission and the other for reception. Hence, propagation-domain isolation techniques can be utilized to reduce self-interference by using a combination of cross-polarization, and antenna directionality.

The total degrees of freedom (DoF) criterion provides a measure of the interference management capability of a network. In most cases, the total DoF is equal to the number of interference-free streams that can be transmitted in the network [5], [6]. Characterizing the DoF of wireless networks with IBFD transceivers has recently received considerable attention, e.g., [7], [8]. The advantages of using separate-antenna IBFD transceivers in cellular networks were investigated in [9], [10]. A single-cell system with multiple mobile nodes was considered in [9] where the base station (BS) is equipped with a separate-antenna full-duplex MIMO transceiver with M_U receive antennas and M_D transmit antennas. In this work, it was shown that the achievable DoF using interference alignment for the full-duplex system is greater than that achieved for a half-duplex system employing $\max\{M_U, M_D\}$ antennas at the BS. The same system was studied in [10] and the DoF was characterized both when the users are half-duplex and full-duplex. However, only a single cell was studied in [7]–[10] and the inter-cell interference was not considered.

Femtocells are low-power access points that are installed by the users to create a small wireless coverage area and connect the user equipment (UE) to the cellular core network. Interference management in heterogeneous networks has been studied extensively in the literature, e.g., see [11] and the references therein. Since femto-BSs are deployed and used privately, unauthorized users can only connect to the macro-BS even if there exists a femto-BS in their vicinity. As a result, severe cross-tier interference might arise if the femto-BS user and the macro-BS user utilize the same frequency band concurrently. Interference alignment was proposed for heterogeneous networks in [12], however, only half-duplex nodes were considered.

In this paper, we consider a heterogeneous network composed of a full-duplex separate-antenna macro-BS and a half-duplex femto-BS that operate in the same frequency band. We assume that the femto-BS utilizes orthogonal resources for transmitting to its users, e.g., using orthogonal frequency division multiple access. On the other hand, the full-duplex macro-BS utilizes the same resource block to transmit to one of its attached downlink users and receive from another user in the uplink. We focus on managing the full-duplex and cross-tier interference to enable the coexistence between the full-duplex macrocell and the femtocell. We assume that the macro-BS is equipped with a separate-antenna full-duplex

This work is funded by a discovery grant from the Natural Sciences and Engineering Research Council (NSERC) of Canada.

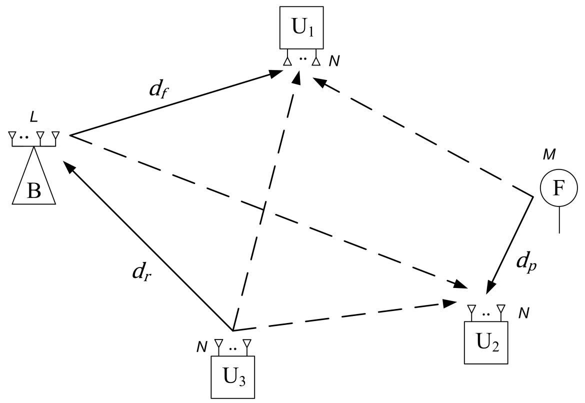

Fig. 1. Heterogeneous network with full-duplex macro-BS, half-duplex femto-BS, and half-duplex UEs. Solid rays represent desired signal transmission while dashed ones represent interference.

transceiver where L_T antennas are used by the macro-BS for downlink transmission while L_R antennas are used for uplink reception and $L_T+L_R \leq L$. We also assume that the femto-BS is equipped with M antennas and that each UE is equipped with N antennas where $L > M \geq N$. To the best of our knowledge, this is the first paper that investigates the DoF of a heterogenous network in which a separate-antenna IBFD transceiver is employed.

We derive several upper bounds on the number of interference-free streams that can be transmitted in the system by using cooperation and message elimination techniques. The derived upper bounds depend on the values of L_T, L_R, M, and N. The optimal antenna allocation, $\{L_T, L_R\}$, at the macro-BS can be found by maximizing the total DoF of the system subject to the derived upper bounds on the number of transmitted interference-free streams. Although this problem is non-convex, we provide an analytical upper bound on the total DoF in terms of L, M, and N only. We utilize interference alignment and zero-forcing beamforming to prove the achievability of the derived upper bound on the total DoF. Based on the ratios M/N and L/N, we propose four different achievability schemes that can attain the upper bound for all values of $L > M \geq N$. We compare the full-duplex system with a half-duplex system in which all the available L antennas at the macro-BS are used only for downlink transmission. We show that full-duplex macro-BS operation can provide DoF gain over half-duplex operation when the number of antennas at the femto-BS is limited, i.e., when $M < 2N$. Hence, full-duplex operation of the macro-BS can be utilized to compensate for the small number of antennas at the femto-BS and increase the number of interference-free streams that can be transmitted in the network.

The remainder of this paper is organized as follows. In Section II, we introduce the system model and the main result of the paper, i.e., the characterization of the DoF of the system. The converse and achievability results are presented, respectively, in Section III and Section IV. Finally, the paper is concluded in Section V.

II. System Model and Main Results

We consider a heterogeneous network composed of a full-duplex macrocell and a half-duplex femtocell operating in the same frequency band as shown in Fig. 1. Similar to the work in [7]–[10], we assume that the self-interference between the transmitting and receiving antennas of the macro-BS is perfectly cancelled. We consider a single time-frequency slot that is used by the macro-BS to transmit the downlink signal to user U_1 and receive the uplink signal from user U_3. The femtocell uses the same time-frequency slot to transmit its downlink signal to user U_2. Let L denote the total number of antennas at the separate-antenna full-duplex macro-BS. We assume that L_T antennas are used for the macrocell downlink transmission to user U_1 while L_R antennas are used for uplink reception from user U_3. The antenna allocation, $\{L_T, L_R\}$, at the macro-BS can be chosen arbitrarily such that $L_T + L_R \leq L$. On the other hand, the femto-BS transmits its downlink signal to its associated user U_2 using M transmit antennas. Let N denote the number of antennas at each UE. We assume that $L > M \geq N$. Due to the limited transmission power of the femto-BS, the femto-BS transmitter does not cause interference at the macro-BS receiver. We assume that the channel between any two nodes is block fading and constant during one time slot and that the channel coefficients are independent, identically distributed and drawn from a continuous distribution. As a result, the channel matrices are independent and full rank almost surely.

Fig. 2 shows the equivalent model for the system under consideration where the transmit and receive sections of the macro-BS have been separated. The resulting system model in Fig. 2 is a partly-connected 3-user MIMO interference channel with feedback. Although the DoF of the 3-user MIMO interference channel has been extensively investigated in the literature, e.g., [6], [13], the DoF of the equivalent system model in Fig. 2 cannot be obtained from any of the readily available results in the literature. In fact, the DoF of the general 3-user MIMO interference channel in which each node is equipped with an arbitrary number of antennas is unknown [13]. In addition, the presence of feedback and partial connectivity in Fig. 2 differentiates the system from the classical 3-user interference channel. The problem is even more complicated due to the variable configuration of the antennas at the macro-BS where L_T and L_R can be chosen to maximize the total DoF.

Let $\mathcal{V}$ denote the set containing the nodes in the system, i.e., $\mathcal{V} = \{B_T, B_R, F, U_1, U_2, U_3\}$ where B_T and B_R respectively denote the transmitter and receiver of the macro-BS while F denotes the femto-BS. Let $W_{Q,P}$ denote the message from node P to node Q where $(Q,P) \in \{(U_1, B_T), (U_2, F), (B_R, U_3)\}$ where the messages are mutually independent. Let $\boldsymbol{H}_{Q,P}$ denote the matrix containing the coefficients of the channel from the transmitter at node P to the receiver at node Q where $P, Q \in \mathcal{V}$ and $P \neq Q$. Let the vector $\boldsymbol{x}_P(n)$ denote the vector transmitted from node $P \in \{B_T, F, U_3\}$ at the nth time slot. The received signals

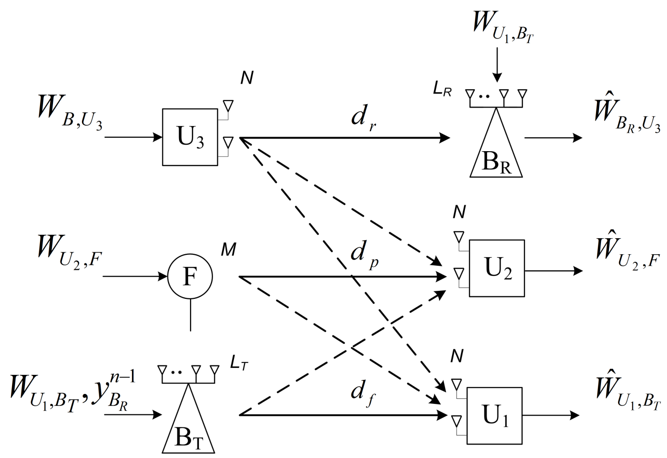

Fig. 2. Equivalent model for the two-cell system in Fig. 1.

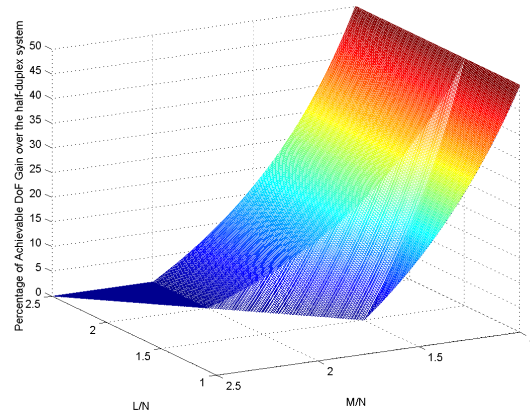

Fig. 3. Relative DoF gain (in percentage) over the half-duplex system for different $L > M \geq N$.

at the macro-BS and the ith user, where $i = 1, 2$, are given respectively by

$$\mathbf{y}_{B_R}(n) = \boldsymbol{H}_{B_R,U_3}\boldsymbol{x}_{U_3}(n) + \boldsymbol{z}_{B_R}(n) \tag{1}$$

$$\mathbf{y}_{U_i}(n) = \sum_{V=B_T,F,U_3} \boldsymbol{H}_{U_i,V}\boldsymbol{x}_V(n) + \boldsymbol{z}_{U_i}(n) \tag{2}$$

where $\boldsymbol{z}_P(n)$ is the additive noise vector received at node P in the nth time slot whose elements are independent and identically distributed circularly symmetric Gaussian random variables with zero-mean and unit-variance.

Let $\mathbf{y}^n_{B_R}$ denote the sequence containing the received signal vectors at the macro-BS from time slot 1 up to time slot n. Since the macro-BS is full-duplex, the encoder function, $\mathcal{E}_{B_T}$, and the decoder function, $\mathcal{D}_{B_R}$ of the macro-BS are given respectively by

$$\boldsymbol{x}_{B_T}(n) = \mathcal{E}_{B_T}\left(W_{U_1,B_T}, \mathbf{y}^{n-1}_{B_R}\right) \tag{3}$$

$$\hat{W}_{B_R,U_3} = \mathcal{D}_{B_R}\left(W_{U_1,B_T}, \mathbf{y}^{D}_{B_R}\right) \tag{4}$$

where D is the length of the transmission block. On the other hand, since the femto-BS and UEs are half-duplex, the encoders (decoders) at these nodes utilize only the desired message (received signals) for encoding (decoding).

In this paper, we characterize the total DoF of the system shown in Fig. 1 which is defined as

$$d_\Sigma = \max_{L_T,L_R} \lim_{\text{SNR}\to\infty} \frac{C(\text{SNR}, L_T, L_R)}{\log(\text{SNR})} \quad \text{subject to } L_T + L_R \leq L \tag{5}$$

where $C(\text{SNR}, L_T, L_R)$ is the total capacity of the network as a function of the SNR for a given antenna allocation $\{L_T, L_R\}$ at the macro-BS [6]. The DoF represents the total number of interference-free streams that can be transmitted from the sources to the destinations. Let us denote the number of streams transmitted from the macro-BS, U_3, and femto-BS by d_f, d_r, and d_p, respectively. As a result, the total DoF of the system is given by $d_\Sigma = d_f + d_r + d_p$. The following theorem presents the main result of the paper.

Theorem 1. *The total DoF of the two-cell heterogeneous network shown in Fig. 1, with separate-antenna full-duplex transceiver at the macro-BS, is given by*

$$d_\Sigma = \max\left\{\frac{3N}{2}, \min\left\{2N, L, \frac{M}{2} + N\right\}\right\} \tag{6}$$

where L, M, and N are the total number of antennas at the macro-BS, the femto-BS, and each UE, respectively, and $L > M \geq N$.

Proof. The converse and achievability proofs for Theorem 1 are provided in Section III and Section IV, respectively. □

Let us compare the DoF achieved by the system when the macro-BS is full-duplex with that achieved when the macro-BS is half-duplex. For the sake of fairness, we assume that the half-duplex macro-BS is equipped with the same total number of antennas as the full-duplex macro-BS. When all the macro-BS antennas are assigned to the downlink[1], the system in Fig. 2 reduces to a two-user MIMO interference channel where B_T transmits to U_1 and F transmits to U_2. In this case, the total DoF of the system is given by $d^{(\text{HD})}_\Sigma$ where

$$d^{(\text{HD})}_\Sigma = d_p + d_f = \min\{M, 2N\}, \tag{7}$$

and is achievable via linear zero-forcing beamforming [5].

The relative DoF gain due to employing full-duplex transceivers at the macro-BS can be defined as $\eta = (d_\Sigma - d^{(\text{HD})}_\Sigma)/d^{(\text{HD})}_\Sigma$. Fig. 3 shows the DoF gain for different values of L/N and M/N. We can see that the full-duplex macro-BS transceiver provides gain over the half-duplex one only when $M < 2N$. In this case, having $L > M$ antennas allows the uplink and downlink of the macrocell to operate simultaneously while managing the resulting interference efficiently. The maximum relative gain occurs when $M = N$ and is equal to 50%.

[1]When the antennas of the half-duplex macro-BS are allocated to the uplink, the interference between the transmitting UE and the receiving one limits the DoF of the system as it reduces to a two-user MIMO Z channel with total DoF given by $d_r + d_p = N$ [14], which is lower than the DoF in (7).

III. Converse Proof of Theorem 1

In this section, we provide the converse proof of Theorem 1. We start by deriving upper bounds on the number of interference-free streams that can be transmitted in the system. We assume that the antenna allocation at the macro-BS is given, i.e., the macro-BS uses L_T antennas for transmission and L_R antennas for reception where $L_T+L_R \leq L$. The upper bound on the DoF of the system can be found by selecting the optimal antenna allocation $\{L_T, L_R\}$ that maximizes the total DoF of the system subject to the derived bounds on the number of transmitted interference-free streams.

First, let us remove the interference links from U_3 on the receiving UEs. This operation cannot decrease the total DoF of the system. The resulting system is composed of two isolated subsystems; a point-to-point link from U_3 to B_R, and a two-user MIMO interference channel containing the downlinks of the two cells. We can also remove the feedback of the message W_{U_1,B_T} at the macro-BS receiver and the output feedback $\mathbf{y}_{B_R}^{n-1}$ at the macro-BS transmitter since the two subsystems are isolated. As a result, we obtain the following bounds on the DoF of the two subsystems [5]

$$
\begin{aligned}
d_r &\leq L_R & (8)\\
d_f + d_p &\leq \min\{2N, M, \max\{L_T, N\}\}. & (9)
\end{aligned}
$$

The third bound on the total DoF of the system can be obtained by eliminating the message $W_{U_2,F}$ and allowing full cooperation between the transmitters of the femto-BS and the macro-BS (forming the node T_1) and full cooperation between the node U_2 and the macro-BS receiver (forming the node T_2). The resulting system is shown in Fig. 4. Note that the interference on node U_2 from B_T can be removed as U_2 has access now to the message transmitted from B_T due to its cooperation with B_R. All the operations described so far cannot reduce the total DoF of the system and therefore do not contradict our upper bound argument [15], [14]. The resulting system in Fig. 4 is a two-user Z-channel with causal output feedback at node T_1 and prior knowledge of message W_{U_1,B_T} at terminal T_2. The DoF of the Z-channel was characterized in [14] where a converse proof was provided that follows the footsteps of the converse proof in [5]. The authors of in [14] started by proving that the sum capacity of the Z-channel is bounded from above by that of the multiple access channel composed of the two transmitters U_3 and T_1 and the receiver U_1 in which the additive noise at U_1 has reduced power compared to the noise at U_1 in the original Z-channel. The proof relies on the ability of the receiver U_1 to decode its intended messages and utilizing the reduction of the noise power at receiver U_1 to enable it to decode the message intended for T_2. As a result, the DoF of the Z-channel is upper bounded by that of the multiple access channel. The same steps of the converse proof in [14] can be repeated in the presence of the message feedback W_{U_1,B_T} at terminal T_2. Hence, it can be shown that the DoF of the system in Fig. 4 cannot be improved beyond that in [14] in spite of the additional feedback. As a result, we obtain the following upper bound

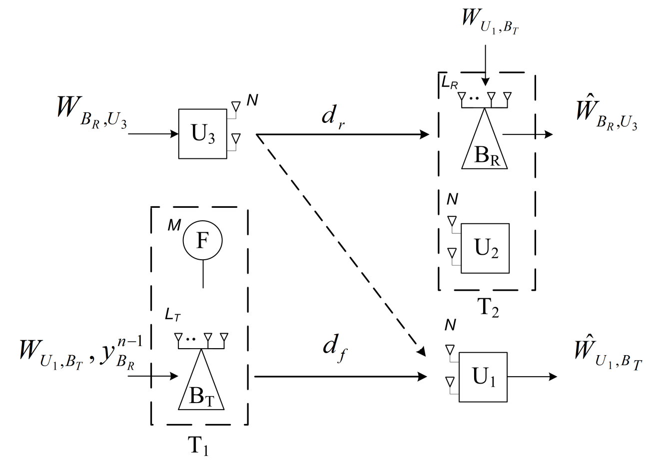

Fig. 4. Resulting system after message reduction and cooperation.

$$d_f + d_r \leq N \tag{10}$$

Similarly, we can eliminate the message W_{U_1,B_T} and allow full cooperation between the transmitters of the femto-BS and the macro-BS and full cooperation between the node U_1 and the macro-BS receiver. The resulting system is a two-user MIMO interference channel whose DoF can be used to bound the DoF of the original system in Fig. 1 by

$$d_p + d_r \leq N. \tag{11}$$

The bounds presented in (8) and (9) depend on the number of transmitting and receiving antennas at the macro-BS. In order to obtain the optimum antenna allocation and the upper bound on the DoF of the system, we maximize the total DoF of the system for a given number of available antennas at the macro-BS under the constraints in (8)–(11). The resulting optimization problem can be written as

$$
\begin{aligned}
\max_{d_f, d_r, d_p, L_T} \quad & d_f + d_r + d_p \\
\text{subject to} \quad & d_f + d_p \leq \min\{2N, M, \max\{L_T, N\}\} \\
& d_r \leq L - L_T \\
& d_f + d_r \leq N \\
& d_p + d_r \leq N \\
& 0 \leq L_T \leq L. \qquad (12)
\end{aligned}
$$

Note that we have substituted for L_R by $L - L_T$ as the additional antennas at the macro-BS receiver will not hurt. The optimization problem in (12) is non-convex due to the $\max\{\cdot\}$ function in the R.H.S. of the first constraint. Note that we have not added an integer constraint on L_T in (12), i.e., we allow fractional values for the number of transmit and receive antennas at the macro-BS. This does not contradict our upper bound argument. Nevertheless, in Section IV we show that we can achieve the DoF obtained from solving (12) by using integer values of L_T and L_R.

In order to solve (12), we divide the non-convex feasible set into two convex subsets and maximize the objective function over each subset. The optimum solution of (12) is obtained by selecting the solution that yields the maximum value of the objective function among the two subproblems. In particular, we divide the feasible set of (12) by using the hyperplane $L_T = N$ into two polyhedrons, and solve the resulting linear program for each subproblem. It can be shown that[2]

$$d_f + d_r + d_p = \begin{cases} \frac{3N}{2} & \text{if } L_T \leq N \\ \min\left\{2N, L, \frac{M}{2} + N\right\} & \text{if } L_T \geq N \end{cases} \quad (13)$$

Hence, the total DoF is bounded by,

$$d_\Sigma \leq \max\left\{\frac{3N}{2}, \min\left\{2N, L, \frac{M}{2} + N\right\}\right\}, \quad (14)$$

which proves the converse of Theorem 1.

IV. Achievability Proof for Theorem 1

In this section, we present the optimal antenna allocation at the macro-BS and the precoders and decoders employed at different nodes that can achieve the upper bound on the total DoF of the heterogenous network in Fig. 1. The proposed achievable schemes employ linear precoding (and decoding) at the transmitting (and receiving) nodes. Let $\boldsymbol{V}_{B_T} \in \mathbb{C}^{L_T \times d_f}$, $\boldsymbol{V}_F \in \mathbb{C}^{M \times d_p}$, and $\boldsymbol{V}_{U_3} \in \mathbb{C}^{N \times d_r}$ denote the precoding matrices at B_T, F, and U_3, respectively. The transmitted signal vector from node P is given by

$$\boldsymbol{x}_P(n) = \boldsymbol{V}_P \boldsymbol{s}_P(n) \quad (15)$$

where $\boldsymbol{s}_P(n)$ is the vector containing the encoded streams of the message transmitted from node P at the nth time slot and $P \in \{B_T, F, U_3\}$. Also, let $\boldsymbol{T}_{B_R} \in \mathbb{C}^{L_R \times d_r}$, $\boldsymbol{T}_{U_2} \in \mathbb{C}^{N \times d_p}$, and $\boldsymbol{T}_{U_1} \in \mathbb{C}^{N \times d_f}$ denote the decoding matrices at B_R, U_2, and U_1, respectively. The received signal vector at node Q is linearly processed by the decoding matrix $\boldsymbol{T}_Q$ to produce an estimate of the encoded streams, i.e.,

$$\hat{\boldsymbol{s}}_P(n) = \boldsymbol{T}_Q^T \mathbf{y}_Q(n) \quad (16)$$

where $(\cdot)^T$ denotes the matrix transpose operator and $(Q, P) \in \{(U_1, B_T), (U_2, F), (B_R, U_3)\}$.

We divide each precoding matrix into several sub-precoders. The interference caused by each sub-precoder can be aligned with the interference from another node at one or more non-targeted receivers, directed towards the nullspace of the channel to a non-targeted receiver, or left uncontrolled. The proposed achievable schemes depend on the ratios between the number of available antennas at the BSs and the number of antennas at each UE, i.e., L/N and M/N. Based on these two ratios, we present four achievable schemes that cover the region $L/N > M/N \geq 1$. Fig. 5 shows the four regions and the achieved DoF in each region.

[2] We will omit the details of the derivation of (13) due to space limitations.

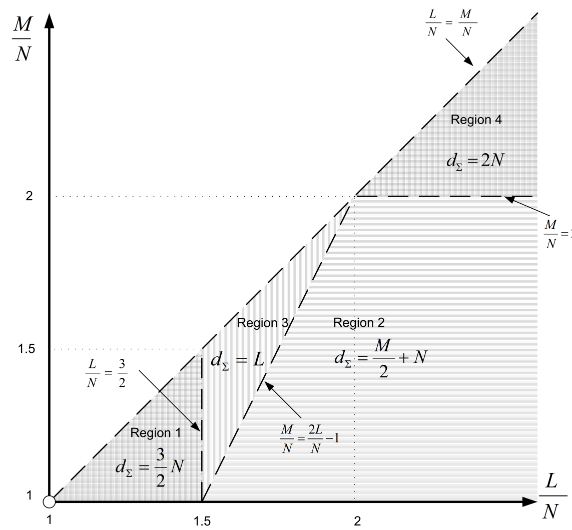

Fig. 5. Total DoF versus L/N and M/N where $L > M \geq N$.

A. Region 1: $L \leq \frac{3N}{2}$

In this region, the upper bound on the total DoF of the network in (14) is given by $d_\Sigma \leq \frac{3N}{2}$. We now proceed to prove that this DoF is achievable. Note that the DoF of the half-duplex system in this region is given by M. In order to achieve the optimal DoF, the antenna allocation at the macro-BS is selected as $L_R = L_T = \lceil \frac{N}{2} \rceil$ where $\lceil x \rceil$ denotes the smallest integer greater than or equal to x. Note that $L - 2\lceil \frac{N}{2} \rceil$ antennas are turned off at the macro-BS, i.e., when N is even only $L = N$ antennas are utilized at the macro-BS while when N is odd only $L = N + 1$ antennas are used. The number of non-interfering streams that can be transmitted in the network in this case is given by $d_f = d_r = d_p = \frac{N}{2}$, and hence, the total DoF of the system is equal to $d_\Sigma = \frac{3N}{2}$. The dimensions of the precoders $\boldsymbol{V}_{B_T}$, $\boldsymbol{V}_F$, and $\boldsymbol{V}_{U_3}$ are given by $\lceil \frac{N}{2} \rceil \times \frac{N}{2}$, $M \times \frac{N}{2}$, and $N \times \frac{N}{2}$, respectively. These precoders are designed such that the interference signals from B_T and U_3 are aligned at U_2 and the interference signals from F and U_3 are aligned at U_1. These two conditions can be written respectively as

$$\boldsymbol{H}_{U_2,U_3} \boldsymbol{V}_{U_3} = \boldsymbol{H}_{U_2,B_T} \boldsymbol{V}_{B_T} \quad (17)$$

$$\boldsymbol{H}_{U_1,U_3} \boldsymbol{V}_{U_3} = \boldsymbol{H}_{U_1,F} \boldsymbol{V}_F. \quad (18)$$

Combining (17) and (18), we can write

$$\left[\boldsymbol{H}_{U_2,U_3}^{-1} \boldsymbol{H}_{U_2,B_T}, -\boldsymbol{H}_{U_1,U_3}^{-1} \boldsymbol{H}_{U_1,F}\right] \begin{bmatrix} \boldsymbol{V}_{B_T} \\ \boldsymbol{V}_F \end{bmatrix} = \mathbf{0}_{N \times \frac{N}{2}} \quad (19)$$

where $\mathbf{0}_{p \times q}$ denotes the $p \times q$ matrix whose entries are zeros. Since the channel matrices are independent and full rank almost surely, the $N \times (L_T + M)$ matrix $\left[\boldsymbol{H}_{U_2,U_3}^{-1} \boldsymbol{H}_{U_2,B_T}, -\boldsymbol{H}_{U_1,U_3}^{-1} \boldsymbol{H}_{U_1,F}\right]$ is also full rank almost surely [6], and the dimension of its null space is given by $M + L_T - N$ which is greater than or equal to $\frac{N}{2}$. Hence, $\boldsymbol{V}_{B_T}$ and $\boldsymbol{V}_F$ can be obtained from (19) and $\boldsymbol{V}_{U_3}$ can be obtained from (17).

Using the precoding matrices $\boldsymbol{V}_{B_T}$, $\boldsymbol{V}_F$, and $\boldsymbol{V}_{U_3}$, the received signals at B_R, U_1, and U_2 are given respectively by

$$\mathbf{y}_{B_R}(n) = \boldsymbol{H}_{B_R,U_3}\boldsymbol{V}_{U_3}\boldsymbol{s}_{U_3}(n) \tag{20}$$
$$\mathbf{y}_{U_1}(n) = \boldsymbol{H}_{U_1,B_T}\boldsymbol{V}_{B_T}\boldsymbol{s}_{B_T}(n) + \boldsymbol{H}_{U_1,U_3}\boldsymbol{V}_{U_3}\left(\boldsymbol{s}_{U_3}(n) + \boldsymbol{s}_F(n)\right) \tag{21}$$
$$\mathbf{y}_{U_2}(n) = \boldsymbol{H}_{U_2,F}\boldsymbol{V}_F\boldsymbol{s}_F(n) + \boldsymbol{H}_{U_2,U_3}\boldsymbol{V}_{U_3}\left(\boldsymbol{s}_{U_3}(n) + \boldsymbol{s}_{B_T}(n)\right) \tag{22}$$

where we have omitted the received noise as the DoF analysis of the system is performed as the SNR goes to infinity. Since the received signal at the macro-BS does not contain any interference, B_R can extract $\boldsymbol{s}_{U_3}(n)$ as $L_R = \lceil \frac{N}{2} \rceil$. Due to our choice of the precoders, the interference is completely aligned at U_1 and U_2 and occupies a subspace of dimension $\frac{N}{2}$ at each receiver. Since U_1 and U_2 are equipped with N antennas each, the desired signal at each node can be extracted by zero-forcing. This completes our achievability proof for this region.

B. Region 2: $L \geq \frac{M}{2} + N, M < 2N$

In this region, the total DoF of the system is bounded by $d_\Sigma \leq \frac{M}{2} + N$. In order to achieve this upper bound, we divide the available antennas at the macro-BS such that $L_T = M$ and $L_R = L - M$. Note that this antenna allocation creates symmetry between the downlinks of the macrocell and femtocell. The precoder matrix at the each BS transmitter is divided into two parts, i.e.,

$$\boldsymbol{V}_{B_T} = \left[\boldsymbol{V}_{B_T}^{(1)}, \boldsymbol{V}_{B_T}^{(2)}\right] \tag{23}$$
$$\boldsymbol{V}_F = \left[\boldsymbol{V}_F^{(1)}, \boldsymbol{V}_F^{(2)}\right] \tag{24}$$

where $\boldsymbol{V}_{B_T}^{(1)}, \boldsymbol{V}_F^{(1)} \in \mathbb{C}^{M \times N - \frac{M}{2}}$ and $\boldsymbol{V}_{B_T}^{(2)}, \boldsymbol{V}_F^{(2)} \in \mathbb{C}^{M \times M - N}$. On the other hand, the precoder at U_3 is given by $\boldsymbol{V}_{U_3} \in \mathbb{C}^{N \times N - \frac{M}{2}}$. The first part of the precoding matrix at each BS is designed to align the interference caused at its non-intended UE with the transmission of $\boldsymbol{V}_{U_3}$ while the second part transmits in the nullspace of the channel to the non-intended UE. These conditions can be written as

$$\boldsymbol{V}_{U_3} = \boldsymbol{H}_{U_2,U_3}^{-1}\boldsymbol{H}_{U_2,B_T}\boldsymbol{V}_{B_T}^{(1)} \tag{25}$$
$$\boldsymbol{V}_{U_3} = \boldsymbol{H}_{U_1,U_3}^{-1}\boldsymbol{H}_{U_1,F}\boldsymbol{V}_F^{(1)} \tag{26}$$
$$\boldsymbol{V}_{B_T}^{(2)} \in \mathcal{N}\{\boldsymbol{H}_{U_2,B_T}\} \tag{27}$$
$$\boldsymbol{V}_F^{(2)} \in \mathcal{N}\{\boldsymbol{H}_{U_1,F}\} \tag{28}$$

where $\mathcal{N}\{\cdot\}$ denotes the nullspace of a matrix. Note that the dimension of the nullspaces of each of $\boldsymbol{H}_{U_2,B_T}$ and $\boldsymbol{H}_{U_1,F}$ is $M - N$, and hence, the nullspace of the channel to the non-intended UE is fully utilized by the transmit precoder of each BS. On the other hand, the dimension of the interference alignment subspace at each receiving UE is given by $N - \frac{M}{2}$. Therefore, $d_p = d_f = N - \frac{M}{2} + M - N = \frac{M}{2}$ and $d_r = N - \frac{M}{2}$.

The above interference alignment conditions for the sub-precoders $\boldsymbol{V}_{B_T}^{(1)}, \boldsymbol{V}_F^{(1)}$ and the precoder matrix $\boldsymbol{V}_{U_3}$ are identical to those for the precoders utilized in Section IV-A. Hence, these matrices can be designed using the same procedure in Section IV-A. This design is always feasible in this region as the dimension of the nullspace of the matrix $\left[\boldsymbol{H}_{U_2,U_3}^{-1}\boldsymbol{H}_{U_2,B_T}, -\boldsymbol{H}_{U_1,U_3}^{-1}\boldsymbol{H}_{U_1,F}\right]$ is $2M - N$ which is always greater than $N - \frac{M}{2}$ since $M \geq N$.

The received signals at B_R, U_1, and U_2 are also given by (20)–(22). At the receiver of the macro-BS, the desired signal is received without any interference. Recall that the number of independent streams transmitted in the uplink of the macrocell is given by $d_r = N - \frac{M}{2}$ and that the macro-BS receiver is equipped by $L_R = L - M$ antennas. The desired signal can be extracted at the macrocell receiver if $d_r \leq L_R$ which is true since $L \geq \frac{M}{2} + N$. On the other hand, at the receiving UEs the dimension of the desired signal is given by $\frac{M}{2}$ while the dimension of the interference subspace is $N - \frac{M}{2}$. Therefore, zero-forcing beamforming can be used to extract the desired signal. For example, the decoding matrix at U_2 is given by

$$\boldsymbol{T}_{U_2} = \boldsymbol{N}_{U_2,U_3}\left(\boldsymbol{V}_F^T\boldsymbol{H}_{U_2,F}^T\boldsymbol{N}_{U_2,U_3}\right)^{-1} \tag{29}$$

where the $N \times \frac{M}{2}$ matrix $\boldsymbol{N}_{U_2,U_3}$ spans the nullspace of the matrix $\boldsymbol{V}_{U_3}^T\boldsymbol{H}_{U_2,U_3}^T$ whose dimension is $(N - \frac{M}{2}) \times N$, i.e., $\boldsymbol{N}_{U_2,U_3}^T\boldsymbol{H}_{U_2,U_3}\boldsymbol{V}_{U_3} = \mathbf{0}_{\frac{M}{2} \times N - \frac{M}{2}}$. Hence, in the absence of noise, the output of the decoding matrix at U_2 is given by

$$\hat{\boldsymbol{s}}_F(n) = \boldsymbol{T}_{U_2}^T\mathbf{y}_{U_2} = \boldsymbol{s}_F(n). \tag{30}$$

Similarly, we can find the decoding matrix $\boldsymbol{T}_{U_1}$ for the macrocell UE. This proves the achievability of $d_p = d_f = \frac{M}{2}$ and $d_r = N - \frac{M}{2}$ DoF, and hence, the total achievable DoF is given by $d_\Sigma = \frac{M}{2} + N$ which coincides with the upper bound on the DoF in this region.

C. Region 3: $L \leq \frac{M}{2} + N, M < 2N$

In this region, the total DoF of the system is smaller than or equal to L. The proposed achievable scheme in this region utilizes the same antenna allocation for the macro-BS as that in Section IV-B, i.e., $L_T = M$ and $L_R = L - M$. However, we use a modified version of the achievable scheme in Section IV-B where the precoders at the transmitting BSs are divided into three parts instead of two, i.e.,

$$\boldsymbol{V}_{B_T} = \left[\boldsymbol{V}_{B_T}^{(1)}, \boldsymbol{V}_{B_T}^{(2)}, \boldsymbol{V}_{B_T}^{(3)}\right] \tag{31}$$
$$\boldsymbol{V}_F = \left[\boldsymbol{V}_F^{(1)}, \boldsymbol{V}_F^{(2)}, \boldsymbol{V}_F^{(3)}\right], \tag{32}$$

while the node U_3 utilizes the precoder $\boldsymbol{V}_{U_3} \in \mathbb{C}^{N \times L - M}$. The sub-precoders $\boldsymbol{V}_{B_T}^{(3)}$ and $\boldsymbol{V}_F^{(3)}$ are selected randomly and the dimension of each matrix is given by $M \times N - L + \frac{M}{2}$ where $N - L + \frac{M}{2} \geq 0$ in this region. On the other hand, the remaining sub-precoders are designed following the same procedure as that in Section IV-B, i.e., using (25)–(28). The dimensions of the sub-precoders $\boldsymbol{V}_{B_T}^{(2)}$ and $\boldsymbol{V}_F^{(2)}$ are also given by $M \times M - N$ as they are designed to transmit in the null-space of the channel to the non-intended UE. However, the dimensions of the matrices $\boldsymbol{V}_{B_T}^{(1)}$ and $\boldsymbol{V}_F^{(1)}$ are selected as $M \times L - M$ as they are designed to align their interference with the interference caused by U_3. Note that this design is feasible as the dimension of the nullspace of the matrix $\left[\boldsymbol{H}_{U_2,U_3}^{-1}\boldsymbol{H}_{U_2,B_T}, -\boldsymbol{H}_{U_1,U_3}^{-1}\boldsymbol{H}_{U_1,F}\right]$ is $2M - N$ which is always greater than $L - M$ in this region.

Using this design for the precoders, the number of transmitted streams in the network is given by $d_p = d_f = \frac{M}{2}$ and $d_r = L - M$. At the receiver of the macro-BS, the desired signal is received without any interference. Since the number of transmitted streams in the uplink of the macro cell is equal to the number of antennas at the receiver of the macro-BS, i.e., $L_R = d_r$, the macrocell can extract its desired streams. On the other hand, the decoders at each receiving UE are designed such that the interference is cancelled via zero-forcing. Note that the proposed scheme divides the available N-dimensional subspace at each receiving UE into three parts; the desired signal subspace which has a dimension equal to $\frac{M}{2}$, the interference alignment subspace (where the interference from the downlink of the interfering BS is aligned with the interference from the uplink of the macro-BS) whose dimension is $L - M$, and the interference subspace where only interference from the interfering BS is received with a dimension $N - L + \frac{M}{2}$. In order to extract the desired signal at U_2, the decoding matrix $\boldsymbol{T}_{U_2}$ is designed according to (29) where $\boldsymbol{N}_{U_2,U_3}$ is given by

$$\boldsymbol{N}_{U_2,U_3} = \mathcal{N}\left\{ \begin{bmatrix} \boldsymbol{V}_{U_3}^T \boldsymbol{H}_{U_2,U_3}^T \\ \boldsymbol{V}_{B_T}^{(3)^T} \boldsymbol{H}_{U_2,B_T}^T \end{bmatrix} \right\} \tag{33}$$

where the dimension of the matrix inside the nullspace operator in the R.H.S. of (33) is $N - \frac{M}{2} \times N$, and hence, its nullspace has a dimension of $\frac{M}{2}$ which is the required dimension for extracting the d_f streams transmitted in the downlink of the femtocell. Similarly, we can find the decoding matrix $\boldsymbol{T}_{U_1}$ for the macrocell UE. This proves the achievability of $d_p = d_f = \frac{M}{2}$ and $d_r = L - M$ DoF, and hence, the total number of achievable DoF is given by $d_\Sigma = L$ which coincides with the upper bound on the DoF in this region.

D. Region 4: $M \geq 2N$

In this region, the DoF of the full-duplex and that of the half-duplex systems are equal to $2N$. Therefore, full-duplex operation of the macro-BS does not yield any gain in the DoF regardless of the number of antennas at the macro-BS. In fact, half-duplex transmission is optimal in this case where $L_T = 2N$, $L_R = 0$, $d_f = d_p = N$ and $d_r = 0$ achieves the upper bound on the DoF of the full-duplex system. The achievable scheme in this case is identical to that in [5] where zero-forcing transmit beamforming is utilized at the femto-BS and macro-BS to steer the transmission in the null space of the channel to the non-intended UE. Note that in this case, the DoF of the system is limited by the number of the antennas at the UEs where all the available N dimensions at U_1 and U_2 are utilized for desired signal reception. Since the number of antennas at U_3 is also given by N, the transmission of U_3 will cause non-avoidable interference at the receiving UEs and will not increase the total DoF of the system beyond that achieved by half-duplex transmission of the macro-BS.

V. Conclusion

We have characterized the DoF gain that can be achieved by using a separate-antenna full-duplex macro-BS in a two-cell heterogeneous network. In particular, we have considered a macro-BS equipped with L antennas where each antenna can be urilized either for downlink transmission or uplink reception and a femto-BS equipped with M antennas that are used for downlink transmission. We have shown that the total DoF of this network is given by $\max\left\{\frac{3N}{2}, \min\left\{2N, L, \frac{M}{2} + N\right\}\right\}$ where N is the number of antennas at each UE and $L > M \geq N$. We have proved the converse of this result using cooperation and message elimination techniques. In addition, we have presented precoding schemes that utilize interference alignment to achieve the total DoF of the system. On the other hand, if all the antennas at the macro-BS were used for downlink transmission, the resulting DoF is given by $\min\{M, 2N\}$. As a result, full-duplex macrocell operation can provide DoF gain over half-duplex operation when the number of antennas at the femto-BS is limited, i.e., when $M < 2N$. The DoF gain reaches 50% when $M/N = 1$.

References

[1] D. Kim, S. Park, H. Ju, and D. Hong, "Transmission capacity of full-duplex-based two-way ad hoc networks with ARQ protocol," *IEEE Transactions on Vehicular Technology*, vol. 63, no. 7, pp. 3167–3183, September 2014.

[2] S. Han, C.-L. I, L. Dai, Q. Sun, and Z. Xu, "Full duplex networking: Mission impossible?," *arXiv: cs.IT/1410.5326*, November 2014.

[3] K. Alexandris, A. Balatsoukas-Stimming, and A. Burg, "Measurement-based characterization of residual self-interference on a full-duplex MIMO testbed," in *Proc. IEEE Sensor Array and Multichannel Signal Processing Workshop*, June 2014, pp. 329–332.

[4] A. Sabharwal, P. Schniter, D. Guo, D.W. Bliss, S. Rangarajan, and R. Wichman, "In-band full-duplex wireless: Challenges and opportunities," *IEEE Journal on Selected Areas in Communications*, vol. 32, no. 9, pp. 1637–1652, September 2014.

[5] S.A. Jafar and M.J. Fakhereddin, "Degrees of freedom for the MIMO interference channel," *IEEE Transactions on Information Theory*, vol. 53, no. 7, pp. 2637–2642, July 2007.

[6] V.R. Cadambe and S.A. Jafar, "Interference alignment and degrees of freedom of the K-user interference channel," *IEEE Transactions on Information Theory*, vol. 54, no. 8, pp. 3425–3441, August 2008.

[7] S.H. Chae and S.H. Lim, "Degrees of freedom of cellular networks: Gain from full-duplex operation at a base station," in *Proc. IEEE Global Communications Conference*, December 2014, pp. 4048–4053.

[8] A. Sahai, S. Diggavi, and A. Sabharwal, "On degrees-of-freedom of full-duplex uplink/downlink channel," in *Proc. IEEE Information Theory Workshop*, September 2013, pp. 1–5.

[9] K. Kim, S.-W. Jeon, and D.K. Kim, "The feasibility of interference alignment for full-duplex MIMO cellular networks," *IEEE Communications Letters*, vol. 19, no. 9, pp. 1500–1503, September 2015.

[10] S.-W. Jeon, S.H. Chae, and S.H. Lim, "Degrees of freedom of full-duplex multiantenna cellular networks," in *Proc. IEEE International Symposium on Information Theory*, June 2015, pp. 869–873.

[11] T. Zahir, K. Arshad, A. Nakata, and K. Moessner, "Interference management in femtocells," *IEEE Communications Surveys Tutorials*, vol. 15, no. 1, pp. 293–311, January 2013.

[12] B. Guler and A. Yener, "Selective interference alignment for MIMO cognitive femtocell networks," *IEEE Journal on Selected Areas in Communications*, vol. 32, no. 3, pp. 439–450, March 2014.

[13] C. Wang, T. Gou, and S.A. Jafar, "Subspace alignment chains and the degrees of freedom of the three-user MIMO interference channel," *IEEE Transactions on Information Theory*, vol. 60, no. 5, pp. 2432–2479, May 2014.

[14] S.A. Jafar and S. Shamai, "Degrees of freedom region of the MIMO X channel," *IEEE Transactions on Information Theory*, vol. 54, no. 1, pp. 151–170, January 2008.

[15] V.R. Cadambe and S.A. Jafar, "Degrees of freedom of wireless networks with relays, feedback, cooperation, and full duplex operation," *IEEE Transactions on Information Theory*, vol. 55, no. 5, pp. 2334–2344, May 2009.